Speed Sensorless Stator Flux-Oriented Control of Induction Motor in the Field Weakening Region Using Luenberger Observer

Tae-Sung Kwon, Myoung-Ho Shin, and Dong-Seok Hyun, *Fellow, IEEE*

***Abstract*—In a conventional speed sensorless stator flux-oriented (SFO) induction motor drive, when the estimated speed is transformed into the sampled-data model using the first-forward difference approximation, the sampled-data model has a modeling error which, in turn, produces an error in the rotor speed estimation. The error included in the estimated speed is removed by the use of a low pass filter (LPF). As the result, the delay of the estimated speed occurs in transients by the use of the LPF. This paper investigates the problem of a conventional speed sensorless SFO system due to the delay of the estimated speed in the field weakening region. In addition, this paper proposes a method to estimate exactly speed by using Luenberger observer. The proposed method is verified by the simulation and experiment with a 5-hp induction motor drive.**

***Index Terms*—Field weakening, induction motor, Kalman filter, Luenberger observer.**

I. Introduction

IN APPLICATIONS such as traction and spindle drive, it is desirable to retain maximum torque capability in the field weakening region. The torque capability of an induction motor is limited by the current rating and the maximum voltage that the inverter can apply to the motor. Many efforts have been made to obtain the maximum torque capability in the field weakening region [1]–[4].

In the speed sensorless stator flux-oriented (SFO) control system, when the estimated speed is transformed into the sampled-data model using the first-forward difference approximation, the sampled-data model has a modeling error which, in turn, produces an error in the rotor speed estimation. The error included in the estimated speed is removed by the use of a low pass filter (LPF) [5]. As the result of that, the delay of the estimated speed occurs in transients by the use of the LPF.

The method for the field weakening operation is to vary the stator flux reference in proportion to $1/\omega_r$. In this method, the base speed for the field weakening operation is determined considering maximum torque capability. In the system with a speed sensor, the appropriate base speed can be determined considering the maximum torque capability. However, in the speed sensorless system, the appropriate base speed could not be determined because of the delay of the estimated speed in transients. Consequently, the inverter runs out of the voltage and the current regulation is lost because of the delay of the onset of the field weakening region owing to the delay of the estimated speed.

To solve this problem, [6] was presented. In this method, the error included in the rotor speed was removed by Kalman Filter and the speed was not delayed in transients. As the result, the current was well regulated in transients in the field weakening region.

This paper presents another method different from [6] to solve the conventional method. This paper investigates the problem of the conventional field weakening method of a speed sensorless SFO system and proposes a new speed estimation scheme to estimate a speed exactly in transients in the field weakening region. The error included in the estimated speed is removed by not a LPF but the Luenberger observer so that the exact speed estimation is achieved in transients. Simulation and experimental results verify the proposed method with a 5-hp induction motor drive [7].

Manuscript received September 9, 2003; revised November 11, 2004. Recommended by Associate Editor B. Fahimi.

T.-S. Kwon is with the Electronic System R & D Center, R & D Division, Korea Automotive Technology Institute, Seoul 330-912, Korea (e-mail: tskwon@katech.re.kr).

M.-H. Shin is with the Department of Electrical Engineering, Seoul National University of Technology, Seoul 139-743, Korea (e-mail: mhshin@snut.ac.kr).

D.-S. Hyun is with the Department of Electrical Engineering, Hanyang University, Seongdong-Ku, Seoul 133-791, Korea (e-mail: dshyun@hanyang.ac.kr).

Digital Object Identifier 10.1109/TPEL.2005.850939

II. Conventional Method

In the conventional SFO system, the field weakening method is to vary the stator flux reference in proportion to the inverse of the rotor speed

$$\lambda_{\rm ds}^{*} = \frac{\omega_b}{\omega_r}\lambda_{\rm ds\_rated}^{*} \tag{1}$$

where `*' = reference value, $\lambda_{\rm ds}$ = d-axis stator flux, $\lambda_{\rm ds\_rated}^{*}$ = rated d-axis stator flux reference, ω_b = base speed, and ω_r = rotor angular speed.

In the speed sensorless SFO system, the estimated rotor speed should be used for the stator flux reference because the speed sensor is not used.

In the SFO system, the estimated synchronous angular speed in stationary α–β reference frame can be given as [8]

$$\hat{\omega}_e = \frac{(v_{\beta s} - R_s i_{\beta s})\hat{\lambda}_{\alpha s} - (v_{\alpha s} - R_s i_{\alpha s})\hat{\lambda}_{\beta s}}{|\lambda_s|^2} \tag{2}$$

where `$\wedge$' = estimated value, R_s = stator resistance; $v_{\alpha s}, v_{\beta s}$ = α and β-axis components of stator voltage; $i_{\alpha s}, i_{\beta s}$ = α and β-axis components of stator current; $\lambda_{\alpha s}, \lambda_{\beta s}$ = α and β-axis components of the stator flux.

The estimated slip angular frequency in rotating d–q reference frame [8], the estimated mechanical rotor speed, and the estimated rotor position can be given as, respectively,

$$\hat{\omega}_{\rm sl} = \frac{(1+\sigma\tau_r p)L_s i_{\rm qs}}{\tau_r(\hat{\lambda}_{\rm ds} - \sigma L_s i_{\rm ds})} \tag{3}$$

$$\hat{\omega}_r = \frac{2}{P}(\hat{\omega}_e - \hat{\omega}_{\rm sl}) \tag{4}$$

$$\hat{\theta}_r = \int \hat{\omega}_r \, dt \tag{5}$$

where $\sigma =$ total leakage factor, $\tau_r =$ rotor time constant, $L_s =$ stator self inductance, $p =$ differential operator, and $P =$ number of poles.

Equation (2) is transformed into the sampled-data model using the first-forward difference approximation. It is noted that the sampled-data model of (2) has a modeling error which, in turn, produces an error in the rotor speed estimation. This error is removed by the use of the LPF of (6). However, the estimated rotor speed is delayed by the use of the LPF in transients. The onset of the field weakening region is also delayed due to the delay of the estimated rotor speed. Consequently, the flux level is very high due to the delay of the onset in transients, so that the inverter runs out of the voltage and the current regulation is lost

$$\hat{\omega}_{r,\rm LPF} = \frac{a}{s+a}\hat{\omega}_r \tag{6}$$

where $-a =$ pole of LPF, $\hat{\omega}_{r,\rm LPF} =$ estimated rotor speed by the use of LPF, and $\hat{\omega}_r =$ estimated rotor speed of (4).

III. Speed Estimation by Luenberger Observer

Dynamic equations can be given as

$$J_m\frac{d\omega_r}{dt} + B_m\omega_r = u + \tau_d \tag{7}$$

$$\omega_r = \frac{d\theta_r}{dt} \tag{8}$$

$$\frac{d\tau_d}{dt} = 0 \tag{9}$$

where $J_m =$ inertia moment, $B_m =$ viscous coefficient, $u =$ driving torque, and $\tau_d =$ load torque.

It is assumed that the load torque τ_d is constant for one sampling period because the load torque is very slowly changed for the sampling period.

State equations can be given as (10) and (11) from (7), (8), and (9)

$$\frac{dx}{dt} = Ax + Bu \tag{10}$$

$$y = Cx \tag{11}$$

where

$$A = \begin{bmatrix} -B_m/J_m & 0 & 1/J_m \\ 1 & 0 & 0 \\ 0 & 0 & 0 \end{bmatrix}, \quad B = \begin{bmatrix} 1/J_m \\ 0 \\ 0 \end{bmatrix}$$

$$C = [0 \quad 1 \quad 0], \quad \text{and} \quad x = [\omega_r \quad \theta_r \quad \tau_d]^T.$$

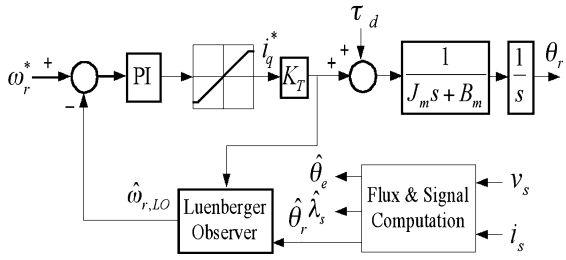

Fig. 1. Block diagram of the speed controller that incorporates the Luenberger observer.

The Luenberger observer uses the errors of the estimated variables compared with the measured variables to correct the errors of the estimated state variables [9]. The Luenberger observer is a dynamical system described by

$$\dot{\hat{x}} = (A - GC)\hat{x} + Bu + Gy = A_o\hat{x} + Bu + Gy \tag{12}$$

where G is the observer gain matrix.

The estimation error $\tilde{x}(t) = x(t) - \hat{x}(t)$ has dynamics given by

$$\dot{\tilde{x}} = (A - GC)\tilde{x} = A_o\tilde{x}. \tag{13}$$

The initial estimation error is $\tilde{x}(0) = x(0) - \hat{x}(0)$ where $\hat{x}(0)$ is the initial value. To ensure that the estimation error vanishes with time for any $\tilde{x}(0)$, we should select the observer gain matrix G so that $A_o = A - GC$ is asymptotically stable. Therefore, the observer gain matrix should be chosen so that all eigenvalues of A_o have negative real parts

$$\mathrm{Re}\{\lambda_j(A_o)\} < 0 \quad j = 1,2,3. \tag{14}$$

When the observer poles are located at $(\lambda_1, \lambda_2, \lambda_3)$, respectively, the following equation can be solved to obtain the G matrix

$$\Delta_o(s) = |sI - A - GC)| = (s-\lambda_1)(s-\lambda_2)(s-\lambda_3) \tag{15}$$

where the $\Delta_o(s)$ is the observer characteristic polynomial.

The observer poles should be located farther from the origin than the poles of the speed control system. If the observer poles are located more close to the origin than the poles of the speed control system, it takes a long time to estimate the actual values of the state variables. However, the control system could be unstable by the measurement noise if the observer poles are located too far from the origin.

The discrete form of (12) can be given as

$$\hat{x}_{k+1} = \Phi_k\hat{x}_k + \Gamma_k(Bu_k + Gy_k) \tag{16}$$

where $\Phi_k = \exp(A_oT)$ and $\Gamma_k = \int_0^T \exp(A_ot)\,dt$.

Fig. 1 shows the block diagram of the speed controller that incorporates the Luenberger observer.

IV. Direct Stator Flux-Oriented System

The control scheme of the proposed drive system is stator flux orientation. Fig. 2 shows the block diagram of the stator flux-oriented control drive that incorporates the proposed scheme. The stator flux magnitude and the transformation angle can be

written as follows from the stator flux in the stationary $\alpha-\beta$ reference frame.

$$|\hat{\lambda}_s| = \hat{\lambda}_{\rm ds} = \sqrt{\hat{\lambda}_{\alpha s}^2 + \hat{\lambda}_{\beta s}^2} \tag{17}$$

$$\cos(\hat{\theta}_e) = \frac{\hat{\lambda}_{\alpha s}}{|\hat{\lambda}_s|}, \quad \sin(\hat{\theta}_e) = \frac{\hat{\lambda}_{\beta s}}{|\hat{\lambda}_s|}. \tag{18}$$

The decoupling compensator is represented in rotating d–q reference frame as (19) [8]

$$i_{\rm dq} = \frac{\hat{\omega}_{\rm sl}\tau_r\sigma i_{\rm qs}}{1+\sigma\tau_r p} = \frac{i_{\rm qs}^2\sigma L_s}{\hat{\lambda}_{\rm ds} - \sigma L_s i_{\rm ds}}. \tag{19}$$

The stator voltage is reconstructed from the inverter switching states [10]. A switching function SA for the phase A is 1 when the upper switch of the phase A is on. The SA is 0 when lower switch of the phase A is on. A similar definition is adopted for the phase B and C. The stator voltage in stationary $\alpha-\beta$ reference frame can be given as

$$v_{\alpha s} = \frac{V_{\rm dc}}{3}(2SA - SB - SC) \tag{20}$$

$$v_{\beta s} = \frac{V_{\rm dc}}{\sqrt{3}}(SB - SC). \tag{21}$$

The processor reads the outputs of the prefilter (LPF, $s = -2985$) through an A/D converter.

The stator flux can be estimated by the integration of the back emf. The stator flux estimation by pure integrator has drift and saturation problems. To solve the problems, in this paper, the following programmable low pass filter is used [4]:

$$\hat{\lambda}_s = \frac{(v_s - R_s i_s)}{s + |\hat{\omega}_e|/3} \frac{\sqrt{\hat{\omega}_e^2 + (\hat{\omega}_e/3)^2}}{|\hat{\omega}_e|} \exp(-j\phi_1) \times \frac{\sqrt{\hat{\omega}_e^2 + 2985^2}}{2985} \exp(j\phi_2) \tag{22}$$

where

$$\cos(\phi_1) = \frac{|\hat{\omega}_e|}{\sqrt{\hat{\omega}_e^2 + (\hat{\omega}_e/3)^2}}$$

$$\sin(\phi_1) = \frac{\hat{\omega}_e/3}{\sqrt{\hat{\omega}_e^2 + (\hat{\omega}_e/3)^2}}, \quad \phi_2 = \tan^{-1}(\hat{\omega}_e/2985).$$

The pole ($|\hat{\omega}_e|/3$) of the programmable LPF is increased to decrease the time constant of the programmable LPF as the speed increase. The constant "3" in $|\hat{\omega}_e|/3$ was selected by trial and error for good performance.

V. Simulation Results

The simulation was carried out with the drive system shown in Fig. 2. The motor parameters are shown in Table I.

Fig. 3 shows the estimated speeds by the Luenberger observer and the LPF when the speed reference is changed from 1000 [rpm] to 4000 [rpm]. The measured speed ω_r is controlled and used for the field weakening operation. The base speed is 1805 [rpm], and the cut off frequency of the Luenberger observer is 60 [rad/s]. With this base speed, it is seen that the current is well regulated in the field weakening region. If the base speed is higher than 1805 [rpm], the inverter runs out of voltage and current regulation is lost. It can be seen that the estimated speed $\hat{\omega}_{r,\rm LPF}$ by the LPF (cut off frequency: 40 [rad/s]) is delayed in transient due to the use of the LPF. However, the estimated speed $\hat{\omega}_{r,\rm LO}$ by the Luenberger observer is not delayed in transient.

Fig. 4 shows the speed and the current when the $\hat{\omega}_{r,\rm LPF}$ is controlled and used for the field weakening operation. At the onset of the field weakening region, the real speed is higher than 1805 [rpm] due to the delay of the estimated speed. As the result, the inverter runs out of voltage, and current regulation is lost.

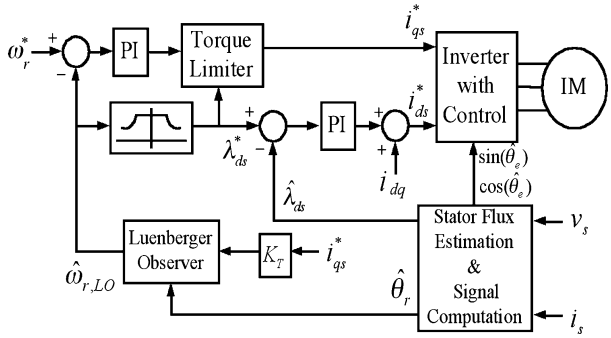

Fig. 2. Block diagram of the stator-flux oriented control drive that incorporates the proposed scheme.

TABLE I
Induction Motor Parameters

3-phase, 5 (hp), 220 (V), 4 (poles), 60 (Hz)		
Rated flux	0.42	(Wb)
Rated line current (peak)	18.2	(A)
Stator resistance	1.26	(Ω)
Rotor resistance	0.2	(Ω)
Magnetizing inductance	50	(mH)
Stator leakage inductance	4.7	(mH)
Rotor leakage inductance	4.7	(mH)
Inertia moment	0.01	(kg·m^2)
Viscous coefficient	0.00001	(N·m·sec/rad)

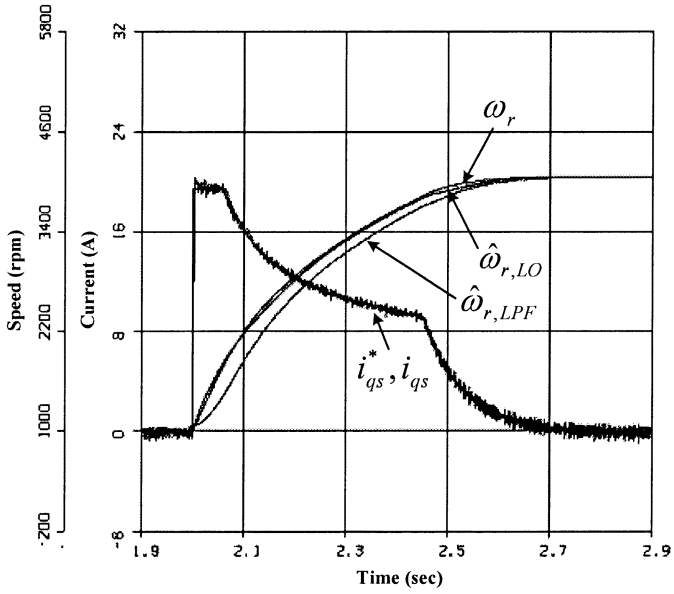

Fig. 3. Estimated speeds $\hat{\omega}_{r,\rm LPF}$ and $\hat{\omega}_{r,\rm LO}$ when the measured speed ω_r is controlled.

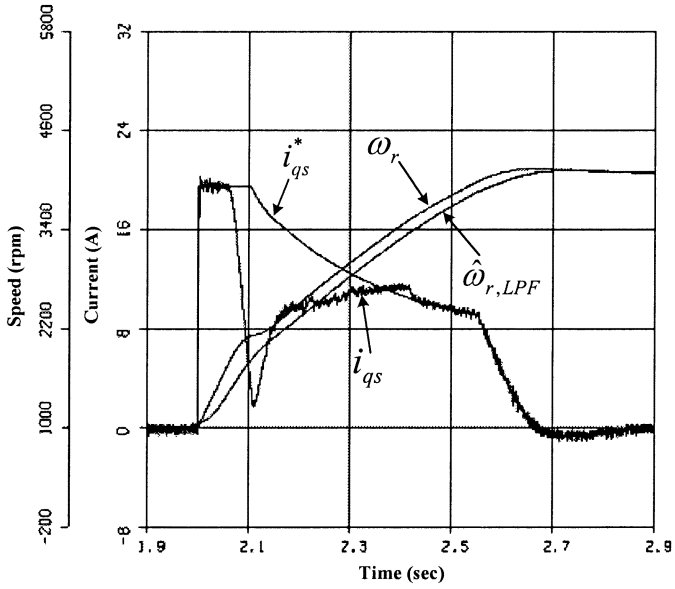

Fig. 4. Speed and current when $\hat{\omega}_{r,\mathrm{LPF}}$ is controlled.

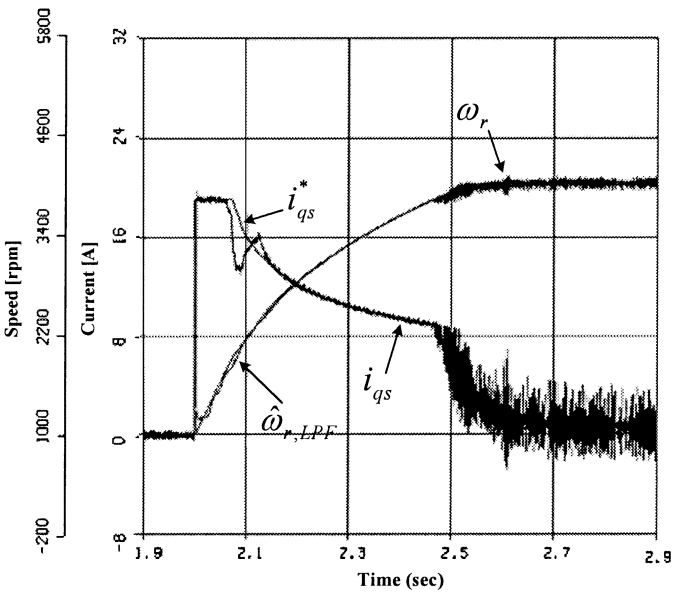

Fig. 5. Speed and current when $\hat{\omega}_{r,\mathrm{LPF}}$ is controlled.

Therefore the torque is reduced and more acceleration time is needed in transient.

Fig. 5 shows the speed and the current when the $\hat{\omega}_{r,\mathrm{LPF}}$ is controlled. The cut off frequency of the LPF is increased in 200 [rad/s] in order to decrease the delay of the estimated speed. In comparison with Fig. 4, the delay of the estimated speed is decreased in transient, but the speed control is deteriorated because the error of the estimated speed is increased.

Fig. 6 shows the speed and the current when $\hat{\omega}_{r,\mathrm{LO}}$ is controlled and used for the field weakening operation. Because the estimated speed $\hat{\omega}_{r,\mathrm{LO}}$ is not delayed in transient, the onset of the field weakening region is not delayed. As the result, it is seen that the current is well regulated.

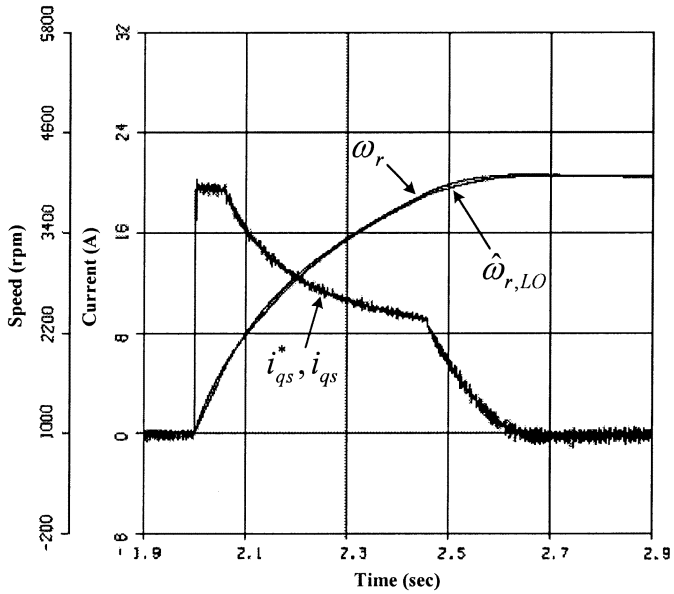

Fig. 6. Speed and current when $\hat{\omega}_{r,\mathrm{LO}}$ is controlled.

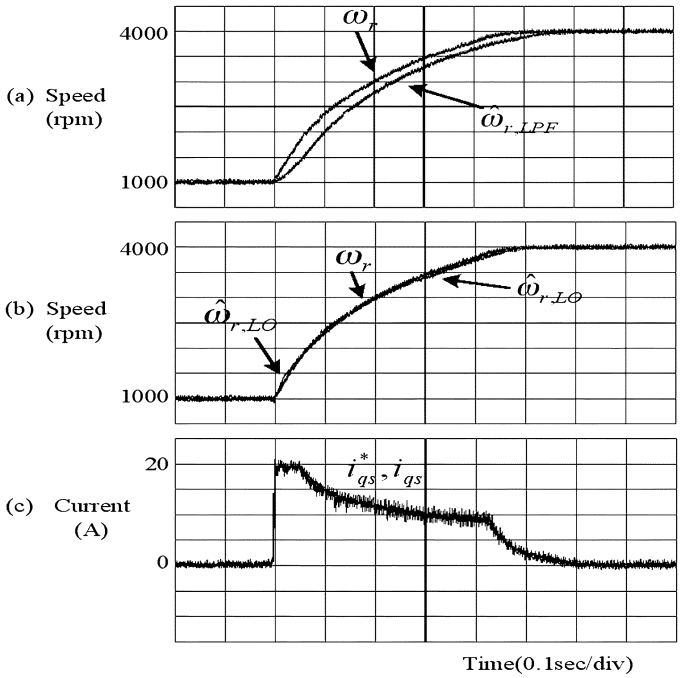

Fig. 7. Speed and current when ω_r is controlled.

VI. Experimental Results

In order to verify the proposed scheme, the control system was implemented by the software of DSP TMS320C31. The inverter input voltage is $V_{\mathrm{dc}} = 325$ [V]. The switching frequency is 4 [kHz]. The current control period is 125 [μs]. The speed control period is 1.25 [ms]. The stator currents are detected through Hall-type sensors. The stator currents are sampled and held at every sampling instant, then A/D converted with 3.5 [μs] conversion time. The Luenberger observer is executed every 125 [μs]. The LPF and the observer pole are all located at -40 [rad/s]. The motor is 5-hp three-phase induction motor shown in Table I.

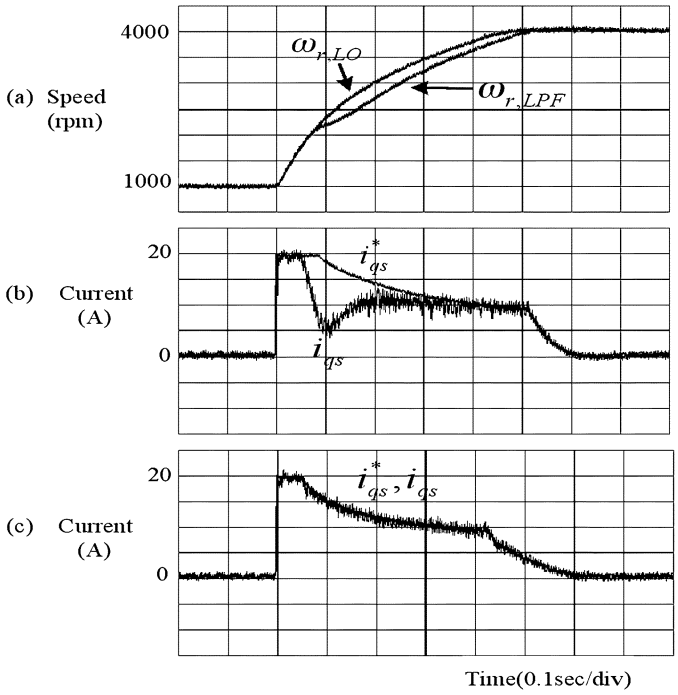

Fig. 8. Measured speeds and currents when $\hat{\omega}_{r,\mathrm{LPF}}$ and $\hat{\omega}_{r,\mathrm{LO}}$ are controlled, respectively.

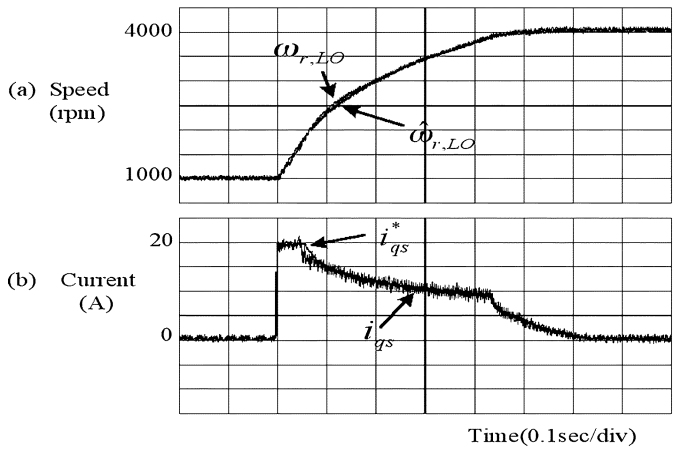

Fig. 9. Speed and current when $\hat{\omega}_{r,\mathrm{LO}}$ is controlled under $+50\%$ inertia moment error and $+200\%$ viscous coefficient error.

Fig. 7 shows the speed and the current when the measured speed is controlled and used for field weakening operation. The base speed is 1805 (rpm). Fig. 7(a) shows the estimated speed $\hat{\omega}_{r,\mathrm{LPF}}$ is delayed in transient due to the use of the LPF. Fig. 7(b) shows the estimated speed $\hat{\omega}_{r,\mathrm{LO}}$ is not delayed in transient. Fig. 7(c) shows that the q-axis current is well regulated.

Fig. 8(a) shows the measured speed $\omega_{r,\mathrm{LPF}}$ and $\omega_{r,\mathrm{LO}}$ when $\hat{\omega}_{r,\mathrm{LPF}}$ and $\hat{\omega}_{r,\mathrm{LO}}$ are controlled, respectively. Fig. 8(b) shows the current when $\hat{\omega}_{r,\mathrm{LPF}}$ is controlled. Fig. 8(c) shows the current when $\hat{\omega}_{r,\mathrm{LO}}$ is controlled. In Fig. 8(b), it is seen that the current regulation is lost since the onset of the field weakening region occurs in the speed higher than 1805 (rpm) due to the delay of the estimated speed $\hat{\omega}_{r,\mathrm{LPF}}$. As the result, in Fig. 8(a), it is seen that the measured speed $\omega_{r,\mathrm{LPF}}$ requires more acceleration time than $\omega_{r,\mathrm{LO}}$.

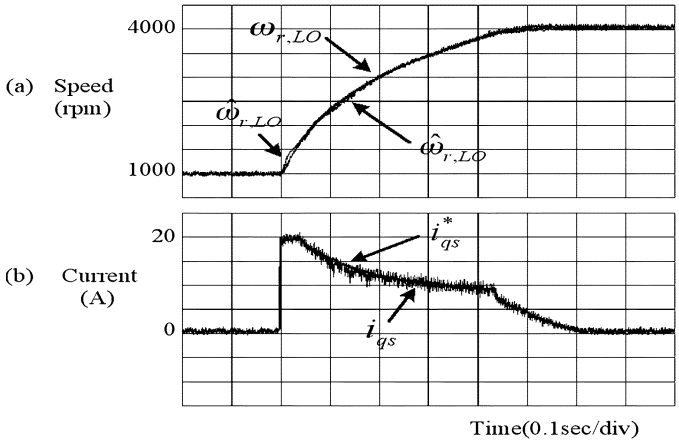

Fig. 10. Speed and current when $\hat{\omega}_{r,\mathrm{LO}}$ is controlled under -50% inertia moment error and $+200\%$ viscous coefficient error.

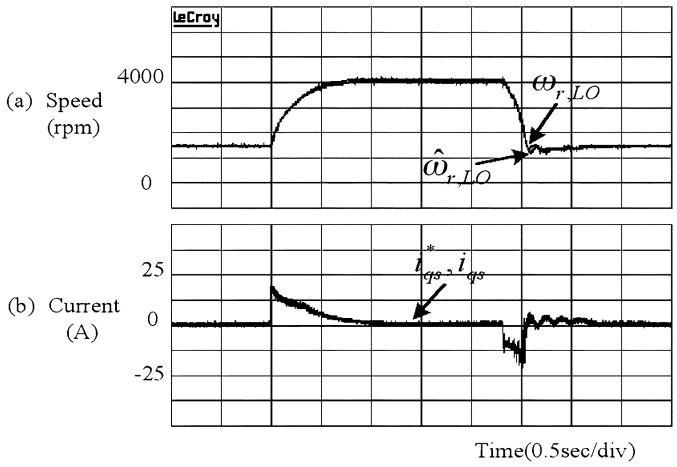

Fig. 11. Speed acceleration and deceleration characteristics of the proposed method.

Fig. 9 shows the speed and current when $\hat{\omega}_{r,\mathrm{LO}}$ is controlled under $+50\%$ inertia moment error (the inertia moment of the motor $=0.01$, the inertia moment of the controller $=0.015$) and $+200\%$ viscous coefficient error (the viscous coefficient of the motor $=0.000\,01$, the viscous coefficient of the controller $=0.000\,03$). The current regulation is lost for a moment at the onset of the field weakening region due to the error of the parameters. However, it is seen that the current is generally well regulated.

Fig. 10 shows speed and current when $\hat{\omega}_{r,\mathrm{LO}}$ is controlled under -50% inertia moment error (the inertia moment of the motor $=0.01$, the inertia moment of the controller $=0.005$) and $+200\%$ viscous coefficient error. It is seen that the performance is not deteriorated at all.

Fig. 11 shows the speed acceleration and deceleration characteristics of the proposed method when the speed reference is changed from 1500 [rpm] to 4000 [rpm] and then changed from 4000 [rpm] to 1500 [rpm]. It can be seen that the speed is well regulated in transients by the proposed method.

Fig. 12 shows the four-quadrant operation characteristics of the proposed method. It is seen that the current control is somewhat unstable close to 0 [rpm]. However it is also seen that the speed is well regulated in transients by the proposed method.

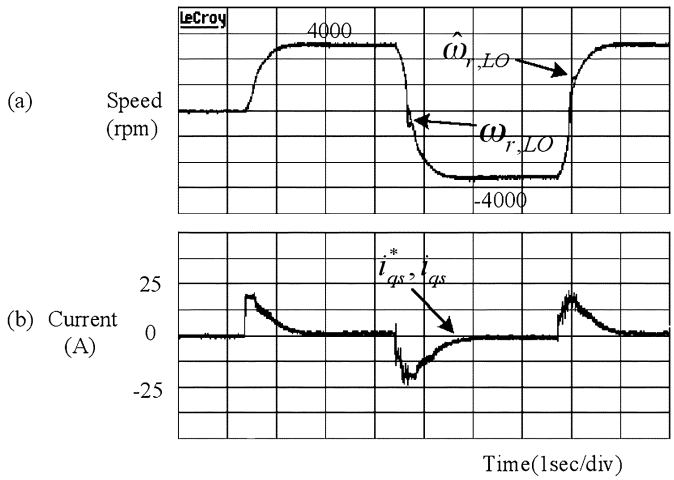

Fig. 12. Four-quadrant operation characteristics of the proposed method.

VII. Conclusion

This paper investigated the problem of the conventional field weakening method of the speed sensorless SFO system and proposed a new speed estimation scheme to estimate speed exactly in transients in the field weakening region. The error included in the estimated rotor speed was removed by not a low pass filter but Luenberger observer.

In the conventional method, the performance in the field weakening region was deteriorated due to the delay of the estimated speed. However, in the proposed method, the estimated speed was not delayed and the performance was not deteriorated in the filed weakening region.

References

[1] X. Xu and D. W. Novotny, "Selection of the flux reference for induction machine drives in the field weakening region," *IEEE Trans. Ind. Applicat.*, vol. 28, no. 6, pp. 1353–1358, Nov./Dec. 1992.

[2] Y. T. Kao and C. H. Liu, "Analysis and design of microprocessor-based vector-controlled induction motor drives," *IEEE Trans. Ind. Electron.*, vol. 39, no. 1, pp. 46–54, Feb. 1992.

[3] S.-H. Kim and S.-K. Sul, "Maximum torque control of an induction machine in the field weakening region," *IEEE Trans. Ind. Applicat.*, vol. 31, no. 4, pp. 787–794, Jul./Aug. 1995.

[4] M.-H. Shin, D.-S. Hyun, and S.-B. Cho, "Maximum torque control of stator flux-oriented induction machine drive in the field weakening region," *IEEE Trans. Ind. Applicat.*, vol. 38, no. 1, pp. 117–122, Jan./Feb. 2002.

[5] L. Ben-Brahim and A. Kawamura, "A fully digitized field-oriented controlled induction motor drive using only current sensors," *IEEE Trans. Ind. Electron.*, vol. 39, no. 3, pp. 241–249, Jun. 1992.

[6] M.-H. Shin and D.-S. Hyun, "Speed sensorless stator flux-oriented control of induction machine in the field weakening region," *IEEE Trans. Power Electron.*, vol. 18, no. 2, pp. 580–586, Mar. 2003.

[7] P. Vas, *Sensorless Vector and Direct Torque Control*. London, U.K.: Oxford University Press, 1998.

[8] X. Xu, R. D. Doncker, and D. W. Novotny, "A stator flux oriented induction machine drive," in *Proc. IEEE Power Electron. Specialists Conf.*, 1988, pp. 870–876.

[9] D. Luenberger, "An introduction to observers," *IEEE Trans. Automat. Contr.*, vol. 16, no. 6, pp. 596–602, Dec. 1971.

[10] T. G. Habetler and D. M. Divan, "Control stategies for direct torque control using discrete pulse modulation," in *Proc. IEEE Industry Applications Soc. Annu. Meeting*, Oct. 1989, pp. 514–522.

Tae-Sung Kwon was born in Seoul, Korea, in 1977. He received the B.S. degree in electrical engineering from Incheon University, Incheon, Korea, in 2002, and M.S. degree in electrical engineering from Hanyang University, Seoul, Korea, in 2004.

He is currently with Korea Automotive Technology Institute, Seoul, where he is a Research Engineer in the Electronic System R & D Center, R & D Division. His research fields are electrical machines, motor drives and energy management system for HEV and EV.

Myoung-Ho Shin was born in Seoul, Korea, in 1967. He received the B.S., M.S., and Ph.D. degrees in electrical engineering from Hanyang University, Seoul, Korea, in 1989, 1991, and 2001, respectively.

From 1991 to 1996, he was with the Samsung Advanced Institute of Technology (SAIT), Suwon, Korea, as a Senior Researcher. He is currently with Seoul National University of Technology where he is an Assistant Professor in the Department of Electrical Engineering. His primary areas of research interest include electrical machines and control systems.

Dong-Seok Hyun (S'79–M'83–SM'91–F'03) received the B.S. and M.S. degrees in electrical engineering from Hanyang University, Seoul, Korea, in 1973 and 1978, respectively, and the Ph.D. degree in electrical engineering from Seoul National University, Seoul, Korea, in 1986.

From 1976 to 1979, he was with the Agency of Defense Development, Korea, as a Researcher. He was a Research Associate in the department of Electrical Engineering, University of Toledo, Toledo, OH, from 1984 to 1985 and a Visiting Professor in the Department of Electrical Engineering, Technical University of Munich, Germany, from 1988 to 1989. Since 1979, he has been with Hanyang University, where he is currently a Professor in the Department of Electrical Engineering and Director of the Advanced Institute of Electrical Engineering and Electronics (AIEE). He is the author of more than 90 publications concerning electric machine design, high-power engineering, power electronics, and motor drives. His research interests include power electronics, motor drives, traction, and their control systems.

Dr. Hyun is a member of the IEEE Power Electronics, Industrial Electronics, Industry Applications, and Electron Devices Societies. He is also a member of the Institution of Electrical Engineers (U.K.), the Korean Institute of Power Electronics, and the Korean Institute of Electrical Engineers.